Available online at www.sciencedirect.com

SCIENCE DIRECT®

Physica B 373 (2006) 306–312

PHYSICA B

www.elsevier.com/locate/physb

Application of the spectral density function method to a composite system

Enis Tuncer[a,*], Nicola Bowler[a], Ian J. Youngs[b]

[a]Center for Nondestructive Evaluation, Iowa State University, Ames, Iowa 50011-3042, USA
[b]Physical Sciences Department, DSTL, Porton Down, Salisbury, Wiltshire, SP4 0JQ, UK

Received 1 December 2005; accepted 1 December 2005

Abstract

The spectral density representation of Bergman [Ann. Phys. 138 (1982) 78] is applied to measurements of bulk permittivity on a composite system with various levels of filler concentration, in order to extract structural information such as shape and spatial arrangement of the filler particles. The composites are paraffin wax filled with metal-coated hollow glass micro-spheres. The inclusions have an outer layer of dielectric which prevents conduction between them. In the spectral density analysis, the dielectric permittivity of the matrix phase is used as measured. The permittivity of the particles is deduced by application of a mixture formula to the measured permittivity of the composite system with low concentrations of filler. The calculated spectral density functions for each concentration level indicate that the topology of the mixtures undergoes a transition when the inclusion concentration reaches approximately 25%.

PACS: 77.22.−d; 77.84.Lf; 02.70.Hm; 02.30.Zz; 02.70.Uu

Keywords: Spectral density function; Dielectric mixtures; Composites; Microwave frequency

1. Introduction

Electrical properties of mixtures have attracted researchers to seek a relation between overall composite properties and intrinsic properties of the parts forming the mixture (constituents) and their spatial arrangement inside the mixture [1–8]. Bergman, in introducing a spectral density function (SDF) for binary mixtures [9–15] proposed that one can separate the geometrical contributions from the pure dielectric response of a composite if and only if the dielectric properties of the constituents are known. Recently, Tuncer [16,17] has shown that the unknown (SDF) in binary mixtures can be determined using a novel numerical technique [18,19], in which constrained least-squares and Monte Carlo techniques are applied simultaneously to solve the ill-posed inversion problem of the spectral density representation (SDR). Here, this method is applied to permittivity data obtained for composite systems consisting of paraffin wax filled with various concentrations of multi-layered spheres, with the aim of extracting topological information about the systems. The filler particles are hollow glass microbubbles [20], first coated with tungsten, then with insulating aluminum oxide. Conductivity across the bulk of the composite is largely prevented, even for high fill factors, by the presence of the aluminum oxide outer layer [21].

The data have been analyzed previously by [22] using a theoretical approach in which the dielectric response of the composites is calculated by an effective medium formula for composites with multi-layered filler particles [23]. In this paper, we determine an effective dielectric permittivity of the filler particles (assumed homogeneous) with an a priori assumption that the effective medium approximations are valid for low concentrations of inclusions. The (SDF) of the system is then extracted by applying the numerical method mentioned above [18,19] and, from this, the structural parameters of the composite system are

---

[*] Corresponding author. High Voltage and Dielectrics, Applied Superconductivity Group, Fusion Energy Division, Oak Ridge National Laboratory, Oak Ridge, TN 37831-6122, USA. Tel.: +1 865 574 0705.

E-mail addresses: enis.tuncer@physics.org, tuncere@ornl.gov (E. Tuncer).

0921-4526/$ - see front matter © 2005 Elsevier B.V. All rights reserved.
doi:10.1016/j.physb.2005.12.001

determined. The calculated SDFs for each filler concentration level indicate that the topology of the mixture undergoes a transition at approximately 25% filler concentration. At concentrations higher than 25%, nearly identical SDFs are determined for high spectral parameters, indicating that these samples have similar topology.

2. Theory

Dielectric properties of mixtures are usually expressed with the help of effective medium theories [1–8]. One such expression is derived for various shapes of inclusions

$$(\varepsilon_e - \varepsilon_m)[\varepsilon_e + (d-1)\varepsilon_m]^{-1} = q(\varepsilon_i - \varepsilon_m)[\varepsilon_i + (d-1)\varepsilon_m]^{-1}, \tag{1}$$

where ε and q are the dielectric permittivity, concentration of inclusions, respectively. The quantity, d, is related to the shape of the inclusions; it is the principle term n of a depolarization tensor of a single ellipsoidal inclusion, $n = d^{-1}$ [2]. Eq. (1) is also known as the Maxwell Garnett approximation [24,25], and for $n = \frac{1}{3}$ it is called Clausius–Mossotti or Maxwell Garnett formula. In a particulated binary composite, n can also take the form of a variable in dilute or isotropic mixtures; e.g. needle-like (prolate) inclusions parallel to the field direction yield $n < \frac{1}{3}$, spherical inclusions yield $n = \frac{1}{3}$, uni-directional cylindrical inclusions perpendicular to the field direction yield $n = \frac{1}{2}$, and oblate inclusions perpendicular to the field yield $n \approx 1$ [26,16]. The subscripts 'e', 'm' and 'i' in Eq. (1) denote the effective medium, matrix and inclusion phases, respectively. Eq. (1) yields the Wiener bounds [27,28] for $d = 1$ and $d = \infty$, corresponding, respectively, to structures layered perpendicular and parallel to the field direction.

A more general representation for the dielectric properties of a mixture is the so-called 'SDR' of Bergman [9–11], where the effective permittivity ε is expressed as [17]

$$\xi \equiv \Delta_{em}/\Delta_{im} = A + \int_{0^+}^{1} g(x)[1 + \varepsilon_m^{-1}\Delta_{im}x]^{-1}\,dx. \tag{2}$$

In Eq. (2), ξ is the complex and frequency-dependent scaled permittivity, $\Delta_{ab} = \varepsilon_a - \varepsilon_b$, and x is the spectral parameter. The constant A depends on both the filler concentration and the structure of the composite, and is related to 'percolation strength'—a measure of conduction due to percolation in the structure [29,30]. The SDF, $g(x)$ in Eq. (2), satisfies the following two relations [11,29,31]:

$$\int_{0^+}^{1} g(x)\,dx + A = q \tag{3}$$

and

$$\int x g(x)\,dx = q(1-q)d^{-1}. \tag{4}$$

These relations connect the SDF directly to the concentration of inclusions and their shape through parameters q and d, respectively.

3. Experiment

Experimental details and sample preparation procedures are published elsewhere [21,22]. The dielectric permittivity of samples was measured on the frequency interval $0.05\,\mathrm{GHz} < \nu < 18.3\,\mathrm{GHz}$. In Fig. 1, the dielectric response of the composites with different inclusion concentration levels q are presented. Nominal and measured values of filler concentration, q_n and $\bar{q}$, respectively, are listed in Table 1. Both the dielectric permittivity ε'_e and losses ε''_e increase with increasing filler concentration. The increase in the real part indicates that the filler has higher dielectric permittivity values than the matrix phase. The structure of the filler particles gives rise to the broad interfacial polarization relaxation peak observed in the data shown in Fig. 1, due to confinement of the conduction electrons in the thin conductive tungsten shell [22]. The tungsten layer is nominally 20 nm thick, although it has been shown by scanning electron microscopy that the layer is not continuous but consists of an approximately uniform distribution of islands with lateral dimension of order 1 μm. Although the dielectric permittivity of the unfilled paraffin wax was measured directly, it was not possible to measure the dielectric permittivity of the inclusion particles, ε_i, independently. Knowledge of ε_i is necessary for application of the SDF analysis. Due to the complicated structure of the inclusions, it is not trivial to determine ε_i. The method by which ε_i was determined is described below.

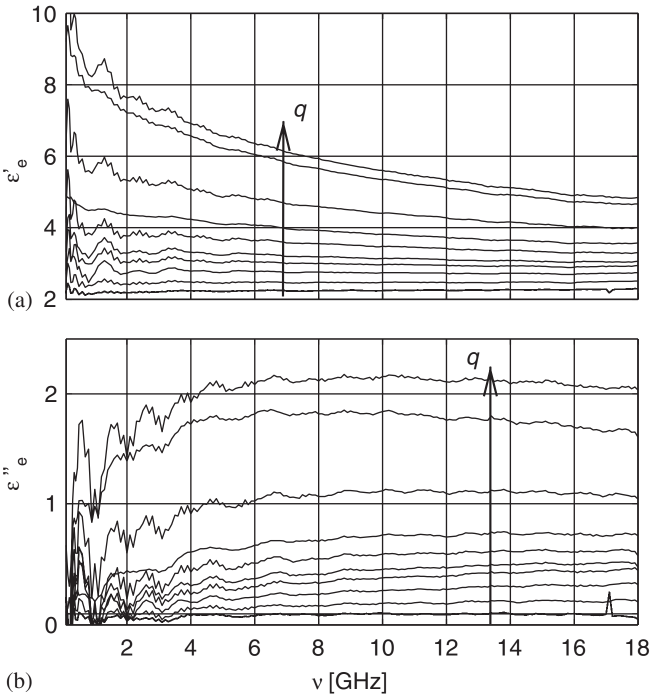

Fig. 1. (a) The real and (b) the imaginary part of the dielectric permittivity ε_e of composites with different filler concentration levels. Nominal and measured values of filler concentration are given in Table 1.

Table 1
Parameters obtained from experiment and spectral density analysis

q_{n}	$\bar{q}$	q_{g}	n^{-1}	x_{gmax}	A	$\varepsilon_{\mathrm{e}}^{\infty}$
0.00	–	–	–	–	–	2.261
0.05	0.07 ± 0.01	0.042	9.1	0.100	0.037	2.472
0.10	0.10 ± 0.02	0.098	4.8	0.220	0.059	2.762
0.15	0.16 ± 0.01	0.152	4.1	0.406	0.078	3.009
0.20	0.23 ± 0.01	0.206	4.5	0.673	0.107	3.208
0.25	0.28 ± 0.01	0.334	4.0	0.931	0.131	3.591
0.30	0.33 ± 0.01	0.404	4.0	0.965	0.169	3.964
0.40	0.45 ± 0.02	0.572	3.5	0.965	0.207	4.686
0.50	0.51 ± 0.02	0.780	3.2	0.931	0.271	5.879
0.55	0.56 ± 0.02	0.639	3.0	0.626	0.261	6.200
1.00	–	–	–	–	–	7.688

q_{n}, $\bar{q}$ and q_{g} are nominal, measured and calculated filler concentrations, respectively. The parameters n and A are related to the shape of the inclusions and percolation arrangements in the structure, respectively. The localization parameter for the most probable spectral density parameter is x_{gmax}. The permittivity of the mixture at high frequencies ($\nu > 16\,\mathrm{GHz}$) is $\varepsilon_{\mathrm{e}}^{\infty}$.

4. Permittivity of the inclusions

First we consider whether the filler particles can be described in terms of an effective dielectric permittivity as illustrated in Fig. 2. For modelling purposes the multi-layer particles are regarded as homogeneous particles exhibiting the same dielectric response as the multi-layer particle. In order to determine the dielectric permittivity of the inclusions we make an a priori assumption, supposing that the effective medium approximations are valid for low concentrations of filler inclusions (in fact, for 5% and 10% filler concentration). The validity is of this assumption is confirmed later in the paper. In Fig. 3, the dielectric permittivities of the matrix (0% filler concentration) and the composite with 5% filler concentration are shown [22]. It can be seen that the losses in the matrix are very small compared to those in the composite. The large deviations and negative loss values in $\varepsilon''_{\mathrm{m}}$ are due to experimental error. Although at first sight, the proposed procedure would look as if it suffers and yields inaccurate results due to lack of higher multipole moments, it is not true since the mixture is a dilute mixture ($q < 0.2$), moreover there are additional reasons to be considered for the studied system. (i) The frequency range is too narrow to detect the influence of multipole moments [32]. (ii) The broadening of the dielectric response due to interaction of particles is not significant—the Debye type relaxation of the interfacial polarization gets only slightly deformed in dense mixtures [5,8]. In addition if multipole moments exist, they would be visible in the spectral density because of their depolarization factors, [33] showed that the distribution of relaxation times in a mixture indicate deviations from that of Debye relaxation in the presence of particle–particle interactions. If the analogy between the distribution of relaxation times and the SDR is taken into account [34], it is clear that the broadening of the dielectric spectrum would be very slightly due to interaction effects. (iii) Finally, if non-ohmic conduction processes exist in the composite system, e.g. hopping or tunneling of charged particles between closely located filler particles, it would be hard to satisfy the conditions for effective medium theories (mixture expressions), and it would also cause the SDR to fail [35,36].

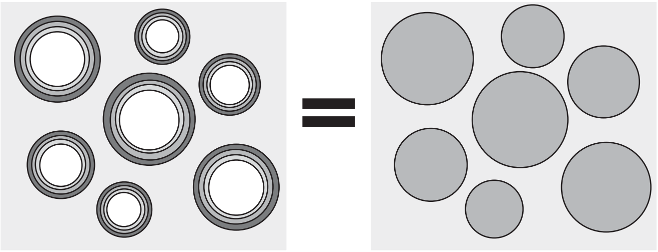

Fig. 2. Visualization of the matrix filled with multi-layered fillers and its equivalent representation as a binary mixture.

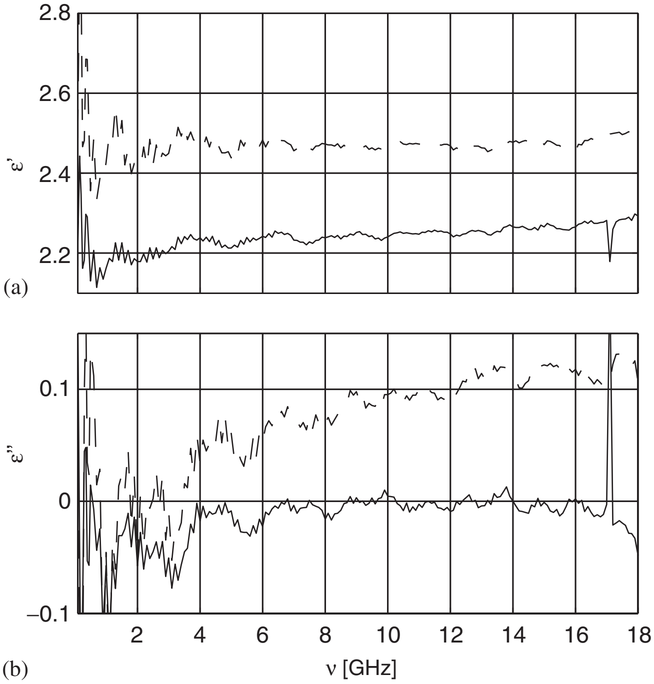

Fig. 3. (a) The real and (b) the imaginary parts of the dielectric permittivity of matrix (——) and composite (- - -) with the lowest concentration level of filler particles studied (5%), respectively.

Proceeding with the above assumption, we use the expression in Eq. (1) and rewrite it for the permittivity of the inclusions ε_{i} as follows:

$$\varepsilon_{\mathrm{i}} = \frac{\varepsilon_{\mathrm{m}}[\varepsilon_{\mathrm{m}}(d-1)(q-1) + \varepsilon_{\mathrm{e}}(d-1+q)]}{\varepsilon_{\mathrm{e}}(q-1) + \varepsilon_{\mathrm{m}}[1+(d-1)q]}. \tag{5}$$

Inserting ε_{e}, measured at $q = 0.05$, and dielectric data of the matrix, ε_{m}, into Eq. (5), one can calculate the permittivity of the inclusions, ε_{i}. The shape factor of the inclusions (n^{-1}) is permitted to be a free parameter in an optimization procedure based on Eqs. (2) and (5). Integration of g with respect to x yields the concentration of the filler particles q, as in Eq. (3).

The optimization procedure yields $d \equiv n^{-1} = 4.8$, corresponding to slightly deformed spheres [37]. The determined permittivity of the filler particles is shown in Fig. 4, and the real part of the permittivity increases with decreasing frequency. The losses indicate a peak occurring at approximately 15.9 GHz, due to Maxwell–Wagner–Sillars polarization effects [26,38,39] at the interfaces between the metal-coating and the dielectric media (aluminum oxide or glass). The dielectric relaxation seen in ε_i may be expressed as a Debye relaxation [40], which has the form

$$\varepsilon_\mathrm{i} - 1 = \Delta\varepsilon(1 + \imath\, 2\pi\nu\tau)^{-1}, \tag{6}$$

with $\Delta\varepsilon$ and τ being the relaxation strength and time, respectively, and $\imath = \sqrt{-1}$. The thick smooth lines in Fig. 4 are generated with $\Delta\varepsilon \simeq 11$ and $\tau \simeq 100\,\mathrm{ns}$.

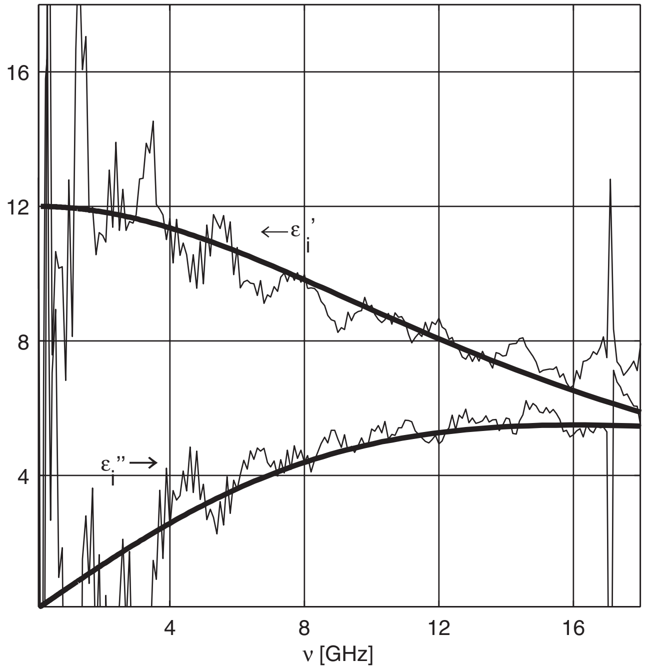

Fig. 4. Dielectric permittivity of inclusions. The thick solid lines are the Debye-type relaxations with $\Delta\varepsilon \simeq 11$ and $\tau \simeq 100\,\mathrm{ns}$.

In order to test whether the calculated permittivity for the inclusions is correct, the Debye-type dispersion presented in Fig. 4 is used to calculate the dielectric permittivity of the composite system with 10% filler concentration, using Eq. (1). In Figs. 5a and b, both the measured and the calculated values of ε_e are presented for $q_\mathrm{n} = 0.10$. Very good agreement is observed. The relative error between the curves is shown in Fig. 5c. Even the ripple due to the experimental error is recovered. We conclude that the procedure adopted here, to determine ε_i for homogeneous particles equivalent to the real multilayered particles by applying effective medium theory to a dilute mixture, is successful.

5. Spectral density function analysis

Now that the permittivities of the inclusions and the matrix are known explicitly, one can proceed to determine the spectral density functions for all of the composite samples. First the composite with 20% filler concentration is considered in detail. In Figs. 6a and b the real and the imaginary parts of the dielectric permittivity for the composite with 20% filler concentration are shown with open symbols (○). For clarity, only every third measurement point is presented in the figure. Since the data has large scatter outside the range ~3−16 GHz (see Fig. 4), only data in this frequency range is used in the numerical analysis. The solid lines in Figs. 6a and b are the values determined with Eq. (2) by inserting the SDF, shown in Fig. 6d. The SDF is extracted from the ratio of the scaled dielectric permittivity values ξ ($\equiv \Delta_\mathrm{em}/\Delta_\mathrm{im}$), shown as an Argand plot in the inset Fig. 6c. The extracted spectral

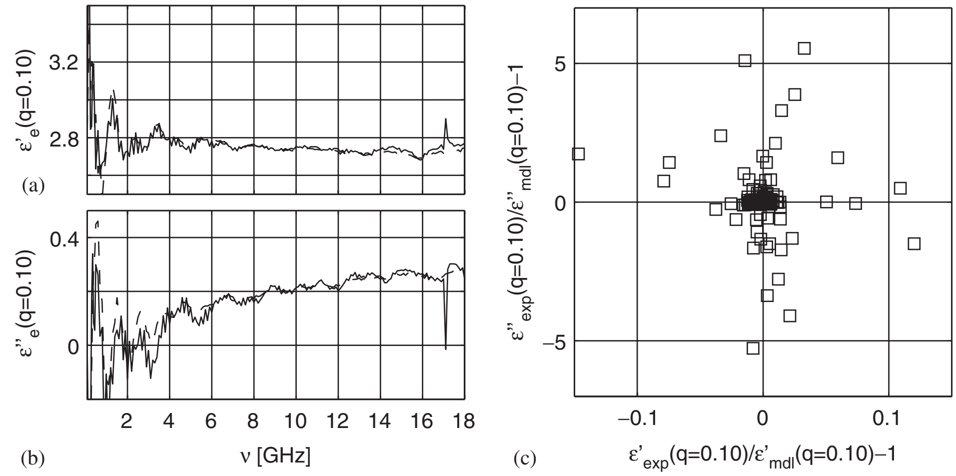

Fig. 5. (a) The real and (b) the imaginary parts of the dielectric permittivity of the composite with 10% filler concentration. The measured and calculated values are presented with dashed (- - -) and solid (——) lines, respectively. (c) The relative error in the calculations.

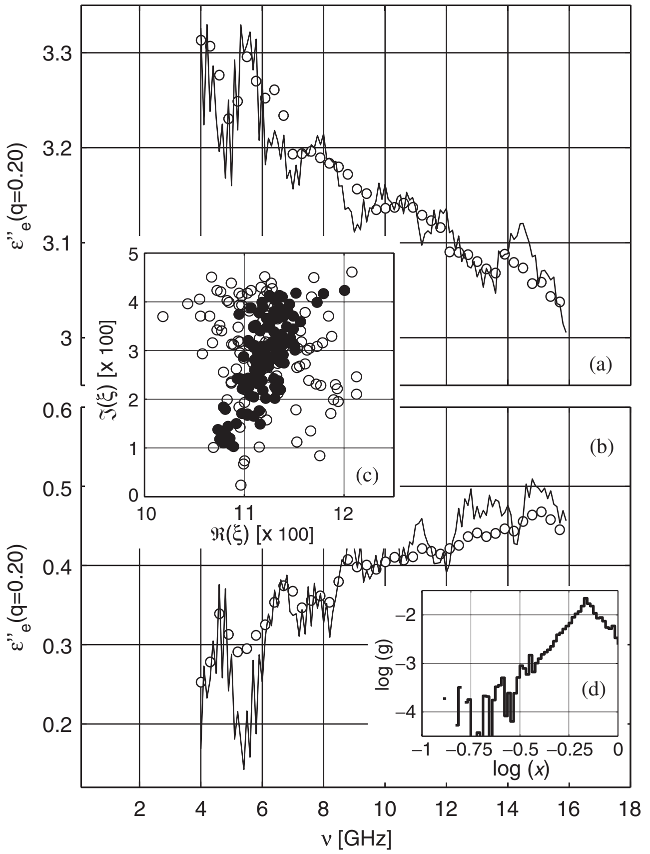

Fig. 6. (a) The real and (b) the imaginary part of the dielectric permittivity of the composite with 20% filler concentration. The solid lines are the results from numerical analysis with the help of Eq. (2). (c) The Argand plot of the scaled dielectric permittivity ξ of the composite with 20% filler. The open (○) and filled (●) symbols represent the measured data and numerical calculations, respectively. (d) The resolved SDFs for the composite.

density function, shown in Fig. 6d, is a delta-sequence [41] with maximum in g at $x_{\mathrm{gmax}} \simeq 0.67$. The integral of g, Eq. (3), results in $q_{\mathrm{g}} \simeq 0.206$ which is close to the measured concentration $\overline{q} = 0.23 \pm 0.01$ given in the description of the sample preparation [21].

The SDFs for all the composite samples, with different filler concentration levels, are presented in Fig. 7. In the figure, the inset shows the most probable spectral parameters as a function of nominal concentration q_{n}. It is clear that the structure of the mixture changes as the concentration rises towards 25%. It is interesting to observe that at concentration levels 25–45% the SDFs are localized around unity, $x_{\mathrm{gmax}} \simeq 1$, and they have similar shape. This indicates that these mixtures are highly homogeneous or the electrical properties of the constituents might have been altered, i.e., influence of non-ohmic conductivity, at these concentration levels. If we assume that the former case is ideal, then the determined structural information is similar for each of these cases and it is not possible to separate differences between the structures as we can for the dilute mixtures [16]. At concentrations of 45% and higher, the SDR (Fig. 7a) indicates additional peaks at lower spectral parameters. These probably indicate the existence of a connected network of filler particles inside the composite, but may indicate the presence of another relaxation process.

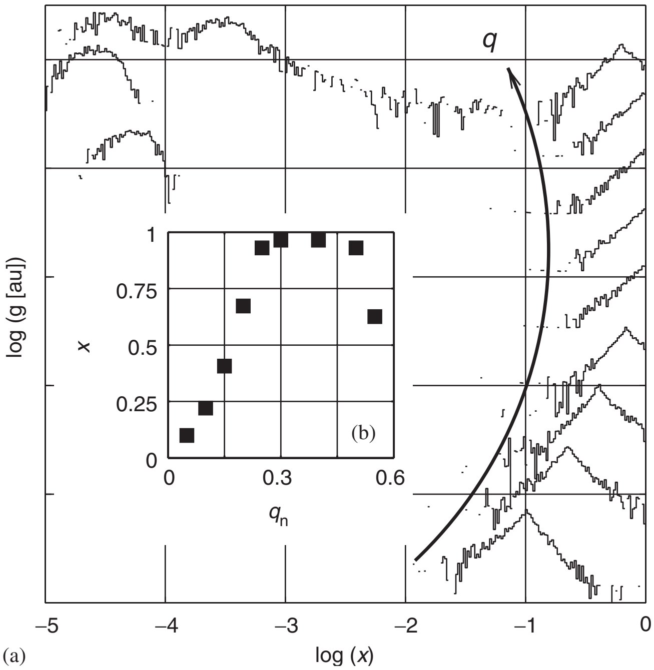

Fig. 7. (a) SDFs of the samples with different filler concentrations, q. (b) The variation of localization parameter x_{gmax} for the spectral parameter g with respect to nominal filler concentration q_{n}.

In Table 1, parameters obtained from the optimization procedure (q_{g} and n) and the SDF analysis (x_{gmax}, A and $\varepsilon_{\mathrm{e}}^{\infty}$—the permittivity of the mixture at frequencies well beyond the influence of the relaxation process) are listed. Plots of the estimated filler concentration q_{g}, the percolation strength A, and the dielectric increment are also shown in Fig. 8 as a function of nominal filler concentration q_{n}.

6. Discussion

Since the inclusions are coated with an insulating outer layer, no significant conduction due to percolation effects is expected. Indeed, the percolation strength A is shown in Fig. 8a to be linear in nominal filler concentration and the slope is $\approx 2^{-1}$. This implies that inter-particle conduction effects have negligible influence on the dielectric properties of these composites because of the insulating dielectric layer on the inclusions, consistent with the experimental observations of Ref. [21].

As seen in Table 1 and Fig. 8a (●), there is very good agreement between q_{g}, q_{n} and $\overline{q}$ for low filler concentrations; $q_{\mathrm{n}} \leqslant 0.20$. For higher concentrations, however, the estimated concentrations are significantly greater (by about 20–50%) than the nominal values. One reason for this could be the existence of aggregates or a connected network of filler particles in the system. Low-frequency permittivity measurements on the same composites suggest

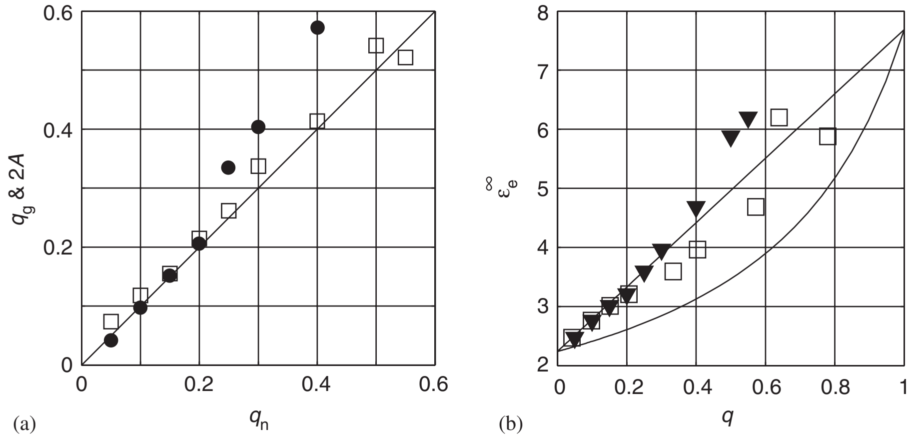

Fig. 8. (a) Both estimated filler concentration q_g (●) and percolation strength A (□) as a function of nominal filler concentration q_n. (b) Dielectric permittivity as a function of nominal concentration q_n (▲) and estimated concentrations by SDR q_g (□). The solid lines (——) in (b) show the Wiener bounds.

that the percolation threshold occurs at around 20% filler concentration [21]. In cases where the particles form connected networks, filler concentrations estimated from the SDF method are likely to deviate from those measured. An other reasonable explanation for this deviation could be the possible increase of the filler or the aggregate conductivity as they approach to each other when the concentration was increased, this may cause tunneling of electrons or hopping of other charge carriers between filler particles that might impose motification of intrinsic filler properties, which were not considered and would be very hard to introduce in the SDR analysis.

The inverse of parameter n, which is related to particle shape, has values listed in Table 1 which range between 3.0 and 4.8 for q_n in the range 0.10–0.55. The composite samples were made using nominally spherical filler particles (for which $n^{-1} = 3$) from the same batch of powder. In fact, n is highly sensitive to particle aspect ratio and $n^{-1} = 4.8$ represents only a slight deformation (elongation parallel to the applied electric field) of a sphere. For example, a prolate spheroid with aspect ratio 2 and long axis parallel to the applied field has $n^{-1} = 9$. Hence we contend that the particle shape is quite well reproduced by the SDF analysis, apart from for the composite with $q_n = 0.05$, in which case $n^{-1} = 9.1$.

In Fig. 8b, the calculated effective dielectric permittivity at high frequencies ($\nu \gg 16\,\mathrm{GHz}$), ε_e^∞, is plotted as a function of filler concentration; both against nominal concentration q_n (▲) and concentration estimated by the SDF method, q_g (□). The Wiener bounds are shown as solid lines. The curve obtained with nominal concentration values appears to violate the Wiener bounds for q_n greater than about 0.30, whereas that obtained with q_g largely obeys the Wiener bounds, except for one concentration value. This observation supports the validity of the concentration values obtained by the SDF analysis, although it is important to note that the position of the Wiener bounds is closely connected to the value of ε_i, about which we have made certain assumptions. If ε_i is actually somewhat larger than the values computed here, then the bounds in Fig. 8b will also shift to larger values of ε_e^∞ and possibly embrace points plotted for both q_n and q_g.

7. Conclusions

In this paper, the SDR method is applied to a particulate composite system consisting of paraffin wax and insulated, metal-coated particles. The a priori assumption made regarding the dielectric permittivity of the filler particles, that effective medium theory applied to composites with low concentrations of inclusions can be used to deduce the dielectric function of the inclusions, was shown to be successful. The SDFs of composites with intermediate filler concentrations (25–45%) were found to be similar, indicating either these samples have similar topological arrangement or the non-ohmic conductivity effects are present that influence the dielectric properties of the constituents. The applied numerical method yields excellent agreement with experimental values when the filler concentration is low, $\leqslant 20\%$. The discrepancies observed between calculated and measured values of filler concentration for values greater than 20%, and the appearance of additional peaks at low spectral parameters for concentrations of 45% and greater, are likely due to the existence of connected networks of filler particles inside the composite, in agreement with low-frequency studies which suggest a percolation threshold of about 20% for this system. Last but not least, the possible presence of non-ohmic conduction processes at concentrations around the percolation threshold and over might have influenced the obtained SDF spectra for those samples with $q \geqslant 20\%$.

As a final note, we attempted to extract the topological description of a composite system by utilizing the SDR method, it is suggested that in future investigations large number of samples will be selected and spectroscopic methods, i.e., optical, scanning electron microscopy, etc., will be used to characterize the samples and their microstructure, which will definitely give better judgement of the SDR method, and its correlation to the composite's topology.

Acknowledgements

N Bowler's work was performed at the Center for NDE at Iowa State University with funding from the Air Force Research Laboratory through S&K Technologies, Inc. on delivery order number 5007-IOWA-001 of the prime contract F09650-00-D-0018. We thank K.P. Lymer and S. Hussain at Future Sytems Technology Division, QinetiQ ltd for performing the high frequency measurements Ian Youngs' contribution was funded by the Ministry of Defence as part of the Emerging and Underpinning Technologies Domain Research Programme.

References

[1] R. Landauer, in: J.C. Garland, D.B. Tanner (Eds.), Electrical Transport and Optical properties of Inhomogeneous Media, AIP Conference Proceedings, vol. 40, American Institute of Physics, New York, 1978, pp. 2–43.
[2] A. Priou (Ed.), Progress in electromagnetics research, Dielectric Properties of Heterogeneous Materials, Elsevier, New York, 1992.
[3] S. Torquato, Random Heterogeneous Materials: Microstructure and Macroscopic Properties, vol. 16, Springer, Berlin, 2001.
[4] M. Sahimi, Heterogeneous Materials I: Linear Transport and Optical Properties, vol. 22, Springer, Berlin, 2003.
[5] E. Tuncer, Y.V. Serdyuk, S.M. Gubanski, IEEE Trans. Dielect. Elect. Insul. 9 (5) (2002) 809 (Preprint cond-mat/0111254).
[6] D.J. Bergman, D. Stroud, Solid State Phys. 46 (1992) 147.
[7] A. Sihvola, Electromagnetic mixing formulas and applications, IEE Electromagnetic Waves Series, vol. 47, The Institute of Electrical Engineers, London, 1999.
[8] E. Tuncer, S.M. Gubański, B. Nettelblad, J. Appl. Phys. 89 (12) (2001) 8092.
[9] D.J. Bergman, Ann. Phys. 138 (1982) 78.
[10] D.J. Bergman, Phys. Rev. Lett. 44 (19) (1980) 1285.
[11] D.J. Bergman, Phys. Rep. 43 (9) (1978) 377.
[12] G.W. Milton, J. Appl. Phys. 52 (1981) 5286.
[13] G.W. Milton, J. Appl. Phys. 52 (8) (1981) 5294.
[14] K. Golden, G. Papanicolaou, Commun. Math. Phys. 90 (1983) 473.
[15] K. Golden, G. Papanicolaou, J. Stat. Phys. 40 (4/5) (1985) 655.
[16] E. Tuncer, J. Phys. D: Appl. Phys. 38 (2005) 223 (Preprint cond-mat/0403468).
[17] E. Tuncer, Phys. Rev. B 71 (2005) 012101 (Preprint cond-mat/0403243).
[18] E. Tuncer, S.M. Gubański, IEEE Trans. Dielect. Elect. Insul. 8 (2001) 310.
[19] E. Tuncer, M. Furlani, B.-E. Mellander, J. Appl. Phys. 95 (6) (2004) 3131.
[20] 3M Product Information, Scotchlite glass bubbles ⟨`http://www.3m.com/microspheres/s_k_1.html`⟩, 2004.
[21] N. Bowler, I.J. Youngs, K.P. Lymer, S. Hussain, in: 2004 Annual Report (IEEE Dielectrics and Electrical Insulation Society, 2004), Conference on Electrical Insulation and Dielectric Phenomena CEIDP, vol. I, pp. 381–384.
[22] I.J. Youngs, N. Bowler, K.P. Lymer, S. Hussain, J. Phys. D: Appl. Phys. 38 (2005) 188.
[23] A.H. Sihvola, I.V. Lindell, in: A. Priou (Ed.), Dielectric Properties of Heterogeneuos Materials, Progress in Electromagnetics Research, Elsevier, Amsterdam, 1992, pp. 101–151.
[24] J.C.M. Garnett, Philos. Trans. R. Soc. London A 203 (1904) 385.
[25] O. Levy, D. Stroud, Phys. Rev. B 56 (13) (1997) 8035.
[26] R. Sillars, J. Inst. Electr. Eng. 80 (1937) 378.
[27] O. Wiener, Der Abhandlungen der Mathematisch-Physischen Klasse der Königl, Sachsischen Gesellschaft der Wissenschaften 32 (1912) 509.
[28] J.L. Greffe, C. Gross, in: A. Priou (Ed.), Dielectric Properties of Heterogeneuos Materials, Progress in Electromagnetics Research, Elsevier, Amsterdam, 1992, pp. 41–100.
[29] K. Ghosh, R. Fuchs, Phys. Rev. B 38 (8) (1988) 5222.
[30] A.R. Day, M.F. Thorpe, J. Phys.: Condens. Matter 11 (1999) 2551.
[31] A.V. Goncharenko, Phys. Rev. E 68 (041108) (2003) 1.
[32] C.R. Snyder, F.I. Mopsik, J. Appl. Phys. 84 (8) (1998) 4421.
[33] E. Tuncer, S.M. Gubański, B. Nettelblad, J. Appl. Phys. 92 (8) (2002) 4612.
[34] E. Tuncer, J. Phys.: Condens. Matter 17 (12) (2005) L125 (`arXiv:cond-mat/0502580`).
[35] G.A. Niklasson, J. Appl. Phys. 57 (1) (1985) 157.
[36] G.A. Gunnar, C.G. Granqvist, J. Appl. Phys. 55 (9) (1984) 3382.
[37] E. Tuncer, S.M. Gubański, Turk. J. Phys. 26 (2002) 1.
[38] J.C. Maxwell, A Treatise on Electricity and Magnetism, third ed., vol. 1, Clarendon Press, Oxford, 1891, reprint by Dover.
[39] K.W. Wagner, Ann. Phys. 40 (5) (1913) 817.
[40] P. Debye, Polar Molecules, Dover Publications, New York, 1945.
[41] E. Butkov, Mathematical Physics, Addison-Wesley Series in Advanced Physics, Addison-Wesley Publishing Company, Menlo Park, 1968.